

# Aerosol spectral optical depths over the Bay of Bengal, Arabian Sea and Indian Ocean

S. K. Satheesh<sup>†,\*</sup>, K. Krishna Moorthy<sup>#</sup> and Indrani Das<sup>‡</sup>

<sup>†</sup>Centre for Atmospheric and Oceanic Sciences, Indian Institute of Science, Bangalore 560 012, India

<sup>#</sup>Space Physics Laboratory, Vikram Sarabhai Space Centre, Thiruvananthapuram 695 022, India

<sup>‡</sup>Meteorology and Oceanography Group, Space Applications Centre, Ahmedabad 380 053, India

Comprehensive investigations during the last decade have clearly established that aerosols have a significant impact on the climate. No serious attempts were made to characterize the aerosols over the Bay of Bengal, despite its role in the regional climate system. This paper reports the results of the measurements of aerosol spectral optical depths made over the Bay of Bengal and compares them with those made over the equatorial Indian Ocean and the Arabian Sea, on-board the oceanographic research vessel, *Sagar Kanya* during its cruise #161-B in March 2001. The aerosol optical depth was found to decrease with distance from the coast with an exponential scale distance of  $\sim 1000$  km for visible wavelengths and  $\sim 1600$  km for near infra-red wavelengths. A significant dominance of small particle concentration near the coast is observed both over the Arabian Sea and the Bay of Bengal. The mean aerosol optical depth was higher over the Bay of Bengal compared to the Arabian Sea, at the shorter wavelengths. Over the equatorial Indian Ocean regions, aerosol optical depths were much lower compared to the Arabian Sea and the Bay of Bengal and showed lesser wavelength dependence. The relative dominance of small particles is more over the Bay of Bengal compared to the Arabian Sea. Back-trajectory analysis shows that during the cruise period, the Arabian Sea was mainly influenced by air masses from the countries lying north-west of India, the Bay of Bengal by air masses from the east coast of India and the equatorial Indian Ocean mostly by the west coast and central India. The observed features are compared with long-term climatology of aerosol optical depth observations from the east and west coast of India and an island station in the Arabian Sea.

In recent years, there has been a substantial increase in interest in the influence of aerosols on the climate, through both direct and indirect effects<sup>1,2</sup>. Many investigators have observed that the aerosol negative forcing downwind of major source regions exceeds the positive forcing due to greenhouse gases<sup>3</sup>. Aerosols alter the magnitude of solar radiation through both scattering and

absorption, also called the *direct effect*. They also enhance the cloud albedo by acting as cloud condensation nuclei and thereby producing an *indirect effect* on radiation.

Aerosols are of natural and anthropogenic origin. On a global scale, the natural sources of aerosols are three to four times larger than the anthropogenic ones, but regionally this factor can change significantly<sup>4-6</sup>. Downwind of major source regions, anthropogenic sources can be as much a factor of three to five times larger compared to natural sources<sup>7</sup>. Although making up only one part in a billion of the mass of the atmosphere, aerosols have the potential to significantly influence the climate. The global impact of aerosol is assessed as the change imposed on planetary radiation measured in  $W m^{-2}$ , which alters the global temperature. Estimation of aerosol radiative forcing is more uncertain than the radiative forcing due to well-mixed greenhouse gases, because of their short lifetimes and the highly inhomogeneous spatial distribution. A description of aerosol forcing with comparable accuracies as that of greenhouse gas forcing requires a better understanding of the aerosol size distribution, chemical composition, vertical distribution and an incorporation of these relevant properties accurately in radiative transfer models. The current estimate<sup>8</sup> of the globally averaged aerosol radiative forcing is about  $-3 W m^{-2}$ , which is comparable with the greenhouse forcing of about  $+2.8 W m^{-2}$ . This may not hold well on a regional scale, especially for regions downwind of major source regions. Aerosol forcing can be even positive in cases where absorbing aerosols are present in sufficient amounts<sup>9</sup>. Although the aerosols have potential climate importance they are poorly characterized in climate models because of the lack of comprehensive database. The international efforts to better understand aerosols include Aerosol Characterization Experiment (ACE-1 and ACE-2)<sup>10,11</sup>, Smoke, Clouds, Aerosols, Radiation-Brazil (SCAR-B)<sup>3</sup>, Tropospheric Aerosol Radiative Forcing Observational Experiment (TARFOX)<sup>12</sup> and the recently concluded Indian Ocean Experiment (INDOEX). The INDOEX was a massive international effort to gather data on aerosols over the tropical Indian Ocean, a data-void region<sup>7</sup>. In India, extensive aerosol

\*For correspondence. (e-mail: satheesh@caos.iisc.ernet.in)

studies are being pursued under the Aerosol Climatology and Effects (ACE) Project of ISRO/DOS-Geosphere Biosphere Programme (GBP), aiming at evolving empirical models of the optical and physical properties of atmospheric aerosols over distinct environments over India<sup>13-15</sup>.

Comprehensive observations conducted during INDOEX and ACE (ISRO-GBP) have resulted in a reasonably good amount of information on aerosols over the Indian subcontinent, the Indian Ocean and the Arabian Sea. The results from the above experiments demonstrated clearly the importance of aerosols on the radiation budget and climate. *What about the Bay of Bengal?* None of these experiments have made measurements over the Bay of Bengal. *In fact the aerosol optical depth measurements over the Bay of Bengal are few or virtually non-existent.* Nevertheless, investigations have shown that the Indian monsoon depends on the Bay of Bengal heat budget<sup>16</sup>. A good part of the rainfall associated with the Indian monsoon is generated by the westward-moving depressions or low-pressure systems in the Bay of Bengal<sup>17</sup>. Despite the important role played by the Bay of Bengal region on the Indian climate and monsoon, no serious observational efforts have been made to make measurements in this region; notwithstanding the understanding of aerosol impact on radiative forcing.

In this paper we present the features of aerosol spectral optical depths ( $\tau_p$ ) estimated over the Bay of Bengal and compare them with similar features over the tropical Indian Ocean and the Arabian Sea. Spectral optical depths are used to infer about the size distribution of aerosols. The results are examined in the light of earlier available knowledge from the ACE (ISRO-GBP) and INDOEX and the implications are discussed.

## Instrument and data

### Aerosol optical depths

The investigations have been carried out on-board the Oceanographic Research Vessel *Sagar Kanya* during its cruise #161-B, which was mainly meant for the validation of the Indian Remote Sensing Satellite, IRS-P4. The instrument used for measuring aerosol spectral optical depths was a multi-spectral hand-held solar radiometer (manufactured by EKO, Japan), which makes measurements at four wavelengths centred at 368, 500, 675 and 778 nm, selected using narrow-band interference filters with band width (full width at half maximum) between 5 and 6 nm (Table 1). The band-selected radiation, after passing through the field-limited optics, is detected using a photodiode. The field of view of the optics is 2.4°. A 'peak hold' facility in the instrument helps to lock to the peak output, thereby enabling meas-

urements from moving and unstable platforms like the ship deck; even under fairly rough sea conditions. The output of the EKO radiometer (obtained as a function of time) has been analysed following the Langley plot method to estimate the total optical depth of the atmospheric column from which aerosol optical depths (defined as the aerosol extinction coefficient integrated over a vertical column of unit cross-section denoted by  $\tau_p$ ) are retrieved using atmospheric models. The details of this standard technique are well documented<sup>18,19</sup> and its application to EKO sun photometer data is discussed elsewhere<sup>13</sup>. A detailed error analysis, considering instrumental and model uncertainties has shown the typical error on the estimate of  $\tau_p$  in the range 0.009 to 0.011 at different wavelengths<sup>20</sup>.

A typical Langley plot obtained for the data on 20 March 2001 (Arabian Sea) is shown in the Figure 1. This method was mainly adopted to eliminate errors due to the deviations or changes in calibration constants of the instrument with time. However, the aerosol optical depths estimated using EKO photometer were compared side by side with measurements with a new calibrated Microtops-II sun photometer (manufactured by Solar Light, Inc., USA) at Bangalore (immediately after the cruise).

**Table 1.** Specifications of photometer filters

Instrument	Wavelength (nm)	Band width (FWHM) (nm)
EKO photometer	368 ± 2	5-6
	500 ± 2	5-6
	675 ± 2	5-6
	778 ± 2	5-6
Microtops-II photometer	340 ± 0.3	2
	380 ± 0.4	4
	500 ± 1.5	10
	675 ± 1.5	10
	875 ± 1.5	10

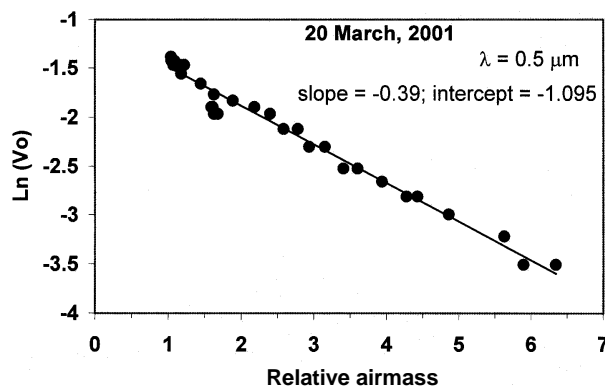


**Figure 1.** Typical Langley plot obtained for the data on 20 March 2001.

Microtops-II is a 5-channel hand-held sun photometer for measuring the aerosol optical depth from individual measurements of direct solar flux, using a set of internal calibration constants. Direct solar radiation at 5 discrete wavelengths is measured. A Global Positioning System (GPS) receiver attached with the photometer provided information on the location, altitude and pressure. The wavelengths are centred about 340, 380, 500, 675 and 875 nm, with a full width half maximum band width of 2 to 10 nm at different wavelengths (Table 1). The field of view of the Microtops radiometer is  $2.5^\circ$ . A comparison of aerosol optical depths from the two instruments has shown a mean difference of  $\sim 0.09$  in aerosol optical depth, at the common wavelength of 500 nm.

The ORV *Sagar Kanya* sailed-off from Chennai on 2 March 2001 and after cruising the Bay of Bengal, the Indian Ocean around the peninsula and the Arabian Sea, reached Goa on 22 March 2001. The cruise track is shown in Figure 2, with circles denoting the position of the ship on the date shown beside. The filled circles correspond to days when spectral optical depths were estimated. Accordingly, aerosol optical depth data were obtained on 18 days. Based on geography and proximity to land, the cruise track is divided into three major sectors as the Bay of Bengal (Sector-I; 2 to 7 March; 6 days of data), the tropical Indian Ocean (Sector-II; 8 to 15 March; 5 days of data) and the coastal Arabian Sea (Sector-III; 16 to 22 March; 7 days of data). The fewer number of days of data over the Indian Ocean is mainly due to the adverse sky conditions during that part of the cruise, close to the equator.

In addition, continuous spectral optical depths were measured using a 10-channel multi-wavelength radiometer (MWR)<sup>19</sup> at the coastal location Trivandrum (TVM in Figure 2) on all clear days and these data have also been used in this study.

### Meteorology

The general synoptic meteorological features over the study area correspond to the transition from the northern winter to spring. The synoptic meteorological conditions during the cruise period were quite similar to those known to prevail over the oceanic regions adjacent to the Indian subcontinent during March<sup>17</sup>. During this period, the synoptic scale winds experienced over this region are mostly low-speed northerlies or northeasterlies; directed from the continental land mass over to the ocean and are associated with the Indian winter monsoon. Rainfall is scanty and the oceanic regions around the peninsula are generally free from any major weather phenomena. The winds gradually start shifting to south-westerlies during April/May, associated with the south-west or summer monsoons. During the present study also there were no major weather systems, except

some weak disturbance south of the equator (when the ship was cruising near the equator). The sky conditions were generally clear and cloud-free for many days. On some days frequent cloud patches were encountered and only few observations were possible. The surface meteorological data (mean wind speed, wind direction, air temperature, relative humidity (RH) and pressure) were obtained at 5 min interval on-board the ship, along with its location in latitude and longitude. All these show features in general conformity with climatologically expected pattern. However, we examine the surface wind fields, as they have the potential to transport aerosols from continent to ocean and vice versa, besides contributing to local production of sea-spray aerosols. In Figure 3, the mean wind vectors are plotted along the cruise track. Each vector is an average for a 6 h period.

In sector-I (Bay of Bengal) rather strong north-westerly winds prevailed, directed from the east coast of India from Chennai to Visakhapatnam. The high-speed winds facilitate rapid transport of nascent continental aerosols to the oceanic regions. It may be borne in mind that the east coast of India is largely industrialized and these winds will carry effluents also along with them. Formation of new sub-micron aerosols is likely to occur over the oceanic environment (which provides ample RH) through secondary (gas-to-particle) production processes and these aerosols will grow by taking water from the ambient oceanic air, which is richer in humidity. The winds become calmer as the ship sails down and then pick up speed in open ocean regions (tropical Indian Ocean; Sector-II). However the winds reaching here can be back-tracked to farther continental regions, i.e. the winds reaching here have a longer sea-travel.

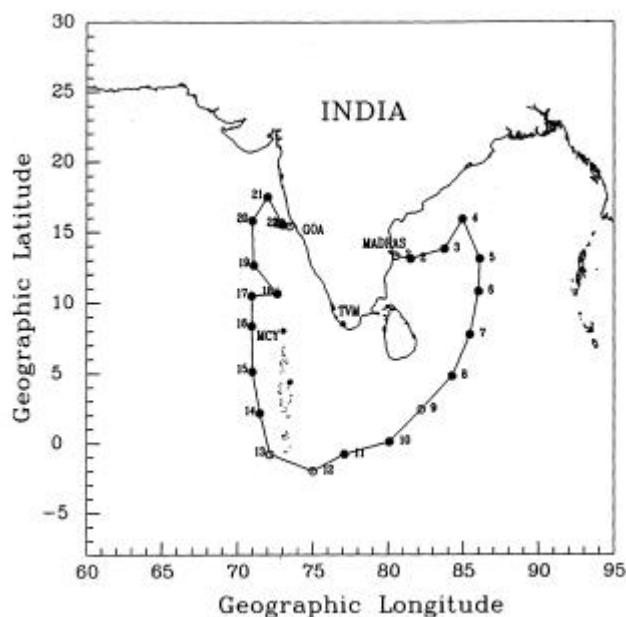


Figure 2. Cruise track of *Sagar Kanya*, cruise # 161-B.

Or in other words, these air masses are not highly influenced by the adjacent continents, as has been the case in Sector-I. Calm easterly winds are encountered in Sector-III (Arabian Sea) till the ship approaches coastal regions of the peninsula. Regions north of  $\sim 8^\circ\text{N}$  experience winds of higher magnitude and coming from various directions, N-W regions of Indian continent, northwest of India, Pakistan and the Gulf countries and also small westerly components traceable backward to northeast regions of Africa. These changing wind patterns will provide corresponding signature in aerosol characteristics, as can be seen in later sections.

*Trajectories*

In addition to the direct surface winds, the air trajectories also assume importance in transport of aerosols and pollutants<sup>13,21,22</sup>. To examine this we have estimated seven-day back-trajectories. The back-trajectories trace the history of air parcels, which influenced the aerosol characteristics at the location of observation, back in time. These were obtained from the Hysplit (Hybrid Single-Particle Lagrangian Integrated Trajectory) model of National Oceanographic and Atmospheric Administration (NOAA). The Hysplit model is the newest version of a complete system for computing simple air-parcel trajectories. Hysplit is a very useful tool to compute the simple forward or backward trajectories. The National Centre for Environmental Prediction (NCEP) runs a series of computer analyses and forecasts, operationally and NOAA's Air Resources Laboratory (ARL) routinely uses NCEP model data for use in air quality transport and dispersion modelling calculations. Typical trajectory plots are given in Figure 4a, b and c, when the ship was cruising over the Bay of Bengal, the Indian

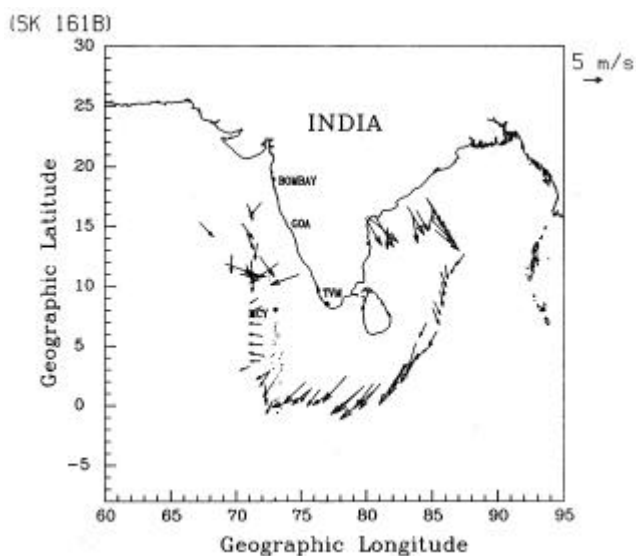


Figure 3. Mean wind vectors plotted along the cruise track.

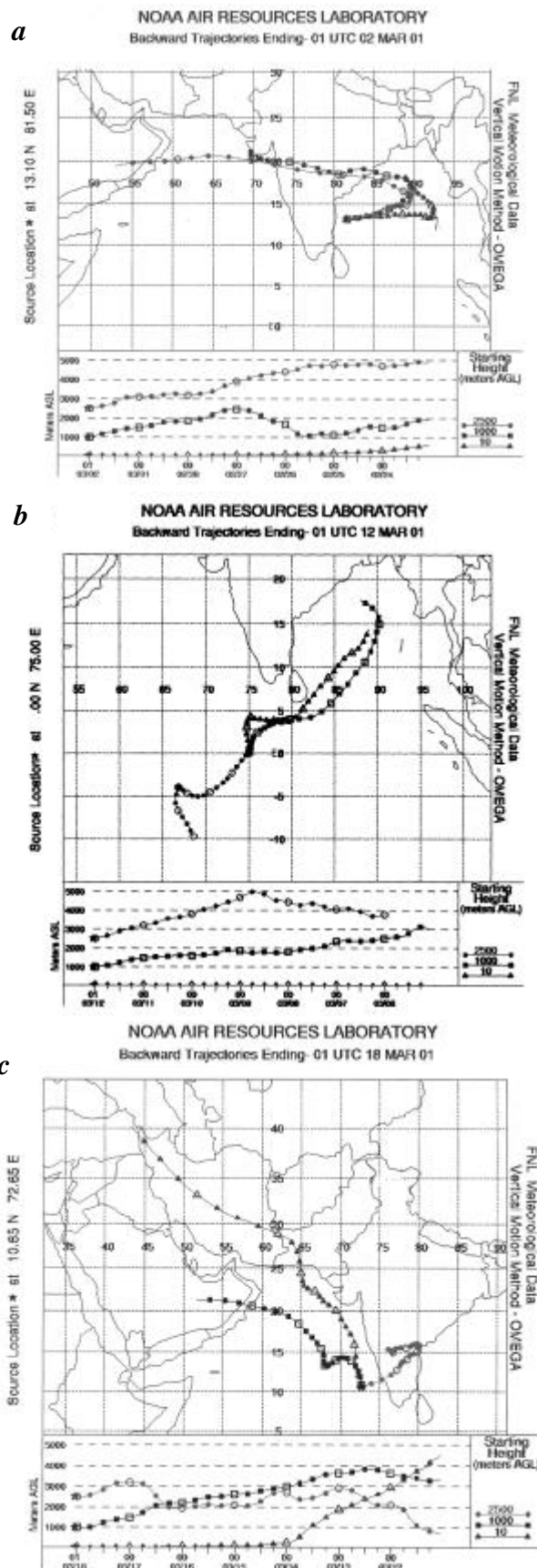


Figure 4. Typical trajectory plots when the ship was cruising over the (a) Bay of Bengal; (b) Indian Ocean; and (c) Arabian Sea.

**Table 2.** Origin of surface air masses encountered during the experiment

Date	Sector	Latitude (°)	Longitude (°)	Air mass
March 2001				
02	I	13.1	81.5	Oceanic; Bay of Bengal
03	I	13.8	83.75	Oceanic; Bay of Bengal
04	I	15.9	84.95	East coast of India
05	I	13.1	86.08	East coast of India
06	I	10.8	86.0	East coast of India
07	I	7.75	85.45	Northeast India; Bangladesh
08	II	4.8	84.25	Central India; Bangladesh
09	II	2.4	82.2	East coast of India; Bangladesh
10	II	0.1	80.08	Sri Lanka; southern India
11	II	0.8	77.1	Bay of Bengal
12	II	-2.0	75.0	Bay of Bengal
13	II	-0.8	72.17	West coast of India
14	II	2.14	71.5	Arabian Sea; northwest India
15	II	5.15	70.99	Arabian Sea
16	III	8.38	70.95	Arabian Sea
17	III	10.5	70.95	Arabian Sea
18	III	10.65	72.65	Northwest India; Arab countries
19	III	12.66	71.09	Northwest India; Arab countries
20	III	15.8	71.0	Arabian Sea
21	III	15.0	72.0	Arabian Sea
22	III	14.5	73.0	Arab countries

Ocean and the Arabian Sea, respectively. The trajectories show that the Bay of Bengal is mostly influenced by the air masses from the central and east coast. The northern Indian Ocean (Sector-II) was also mostly influenced (at least during the cruise period) by the same air masses, which originated from the east coast of India, but had a much longer sea-travel. The Arabian Sea (Sector-III) on the other hand, was influenced by air masses originating from the regions northwest of the Indian continent. On some occasions air mass from the Indian region also passed over the Arabian Sea. A detailed day-by-day back-trajectory analysis is given in Table 2. The general features of the trajectories are similar to those of the surface winds shown in Figure 3, suggesting a rather stable meteorological condition during the cruise.

## Results and discussion

### *Spatial gradients*

The temporal variations of aerosol optical depth,  $\tau_p$ , at three wavelengths (near UV, visible and near IR) are shown in Figure 5. On examining along with the cruise track in Figure 2, the three sectors are clearly discernable with distinct optical depths characteristics. High optical depths are encountered at both the UV and visible wavelength (368 and 500 nm) in both Sector-I and Sector-III, while the tropical Indian Ocean (Sector-II) shows distinctly lower values. It can also be noticed that there is, in general, a decrease in  $\tau_p$  with distance from the coast. A decrease in  $\tau_p$  at the visible wavelengths from about 0.6 to 0.2 and near IR wavelengths from 0.3

to 0.2 was observed from Sector-I to Sector-II. If we assume an exponential decrease in  $\tau_p$  with distance estimated along the mean wind direction following the previous investigations<sup>23</sup>, the *scale distance* for visible wavelength aerosol optical depth is about 1000 km and for near IR aerosol optical depth is about 1600 km. This is because the decrease is more significant at shorter wavelengths (due to reduced source impacts), while at the longer wavelengths the decrease is not very significant, as local production of sea-spray aerosols by the strong surface winds partly replenishes the loss<sup>23</sup>. In this estimation, the measurements over the Arabian Sea are not included since as the trajectories show, their origin is not mostly from the nearest continent (India), but from other locations also.

The spatial variation of aerosol optical depths over the Arabian Sea and the Indian Ocean has been studied in the past<sup>19,23</sup>, when the synoptic scale winds were from the Indian subcontinent. A *scale distance* in the range ~1700 to 2400 km at different wavelengths was reported. During subsequent investigations in 1998 and 1999, the *scale distance* was found to be ~1200 km (ref. 24) and especially shorter scale distance was encountered when near-coastal optical depths were higher. Over the Bay of Bengal, a smaller value for the scale distance is indicated. This means that either the residence time of the aerosols found over the Bay of Bengal is less compared to that over the Arabian Sea or the near-coastal optical depths are higher. Another possibility is that the transport mechanism may not be as efficient over the Bay of Bengal as over the Arabian Sea. Moreover the present cruise was confined more to

tropical locations, whereas the INDOEX cruises reached farther oceanic regions.

*Size distribution*

It is well known that aerosol spectral optical depths contain information pertaining to their size distribution. Following the inverse power law representation of the spectral variation of aerosol optical depth of Angstrom<sup>25</sup>,

$$\tau_p = b\lambda^{-a} \tag{1}$$

where  $a$  is the wavelength exponent,  $b$  is the turbidity parameter (Angstrom coefficient) and  $\lambda$  is the wavelength in  $\mu\text{m}$ . The value of  $a$  depends on the ratio of the concentration of large to small aerosols and  $b$  represents the total aerosol loading in the atmosphere<sup>18</sup>. For the case where the aerosol number size distribution follows the inverse power law form

$$n(r) = n_0 r^{-g} \tag{2}$$

where  $n(r)$  is the number concentration of aerosols in an infinitesimal radius  $dr$  centred at  $r$ ,  $n_0(r)$  is a constant depending on the total aerosol concentration and  $g$  is the power-law index,  $a$  and  $g$  are related through the expression

$$g = a + 3. \tag{3}$$

Higher values of  $a$  thus indicate a sharper aerosol size spectrum, more dominated by smaller aerosols. The values of  $a$  and  $b$  are obtained by linear least square fitting of  $\tau_p - \lambda$  estimates on a log-log scale. For this, we have used sector mean values of  $\tau_p$ . These are obtained by averaging the individual mean values of  $\tau_p$  falling within each sector considered in this study.

Evolving a least square fit of these  $\tau_p - \lambda$  values to eq. (1),  $a$  and  $b$  are estimated separately for each of the three sectors (Figure 6a and b). Relatively higher

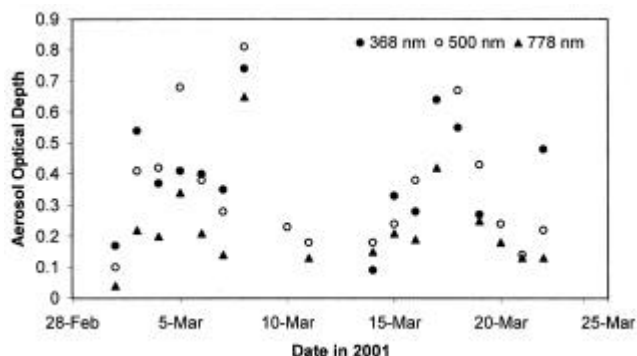


**Figure 5.** Temporal variations of aerosol optical depth at three wavelengths (near UV, visible and near IR).

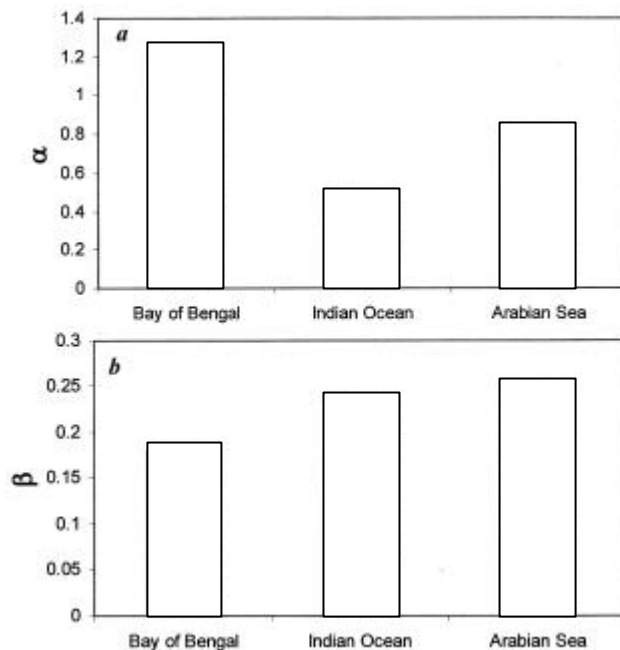


**Figure 6.** Mean values of (a),  $a$  and (b)  $b$  separately, for each of the three sectors.

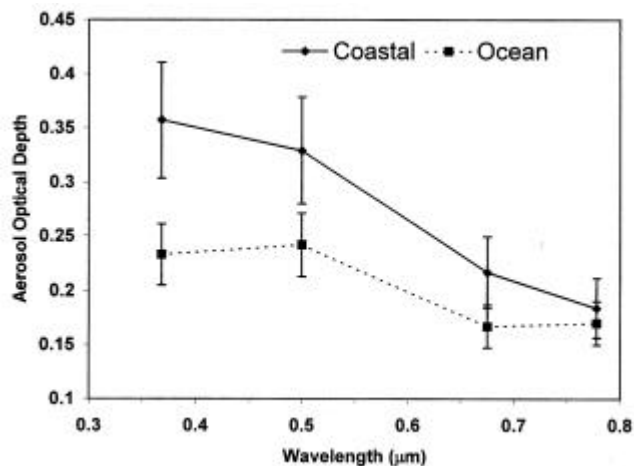


**Figure 7.** Spectral variation of aerosol optical depth averaged over near-coastal and oceanic regions.

dominance of small particles is observed both over the Bay of Bengal and the Arabian Sea sectors compared to the Indian Ocean sector, as indicated by the higher values of  $a$ . The value of  $a$  over the Indian Ocean sector is less than half the value over the Bay of Bengal. Examining this with the optical depth values shown in Figure 5, it is evident that this decrease in  $a$  over the Indian Ocean is caused more by the rapid decrease in aerosol optical depth at the shorter wavelengths than at longer wavelengths, where  $\tau_p$  remains more or less around the same value. This indicates that the fine sub-micron aerosols contributing to  $\tau_p$  at shorter wavelengths are more of continental origin and dominate over the oceanic regions of the east and west coast. But as we move

further away, their concentration decreases due to reduced impact of the sources, as there are no significant sources of these fine aerosols over the ocean. On the other hand, a major share of large super-micron aerosols is produced rather locally over the ocean surface by sea-spray<sup>23</sup> and hence their abundance does not decrease as rapidly (as also seen from the higher value of scale distance). Consequently, the size spectrum broadens and  $a$  decreases. A nearly flat optical depth spectrum is typical to pristine ocean environments, as has been shown during the INDOEX studies<sup>13,19</sup>. This is further corroborated by the almost similar values for  $b$  over all the three sectors (Figure 6b). As  $b$  is more sensitive to super-micron aerosols, the above observation indicates that the concentration of larger particles does not show significant spatial variations. However, there is a significant enhancement in the concentration of sub-micron aerosols in the near-coastal regions and the decrease as the ship moves away from the coast is sharp. Further, it is also seen that the value of  $a$  is higher over the Bay of Bengal than over the Arabian Sea.

The size distribution of aerosols over the Arabian Sea and the Indian Ocean has been studied in detail by Moorthy *et al.*<sup>26</sup>. Also in a simple way (using the Angstrom parameters), the size characteristics over the Arabian Sea are reported in Satheesh and Moorthy<sup>20</sup>. The value of  $a$  reported by them for the Arabian Sea ranges from 1.2 for near-coastal regions to 0.6 in remote oceanic regions. In the present study, the value of  $a$  for near-coastal regions of the Arabian Sea is about 1.2 and is consistent with the above findings.

As the cruise was confined only to the coastal region, the study cannot be extended to deeper oceanic regions. The mean value of  $a$  for the Arabian Sea is about 0.8, which is in agreement with the previous values. For the Bay of Bengal, the near coastal value is as high as 1.8. The mean value for the Bay of Bengal is about 1.2. This implies that the Bay of Bengal region has a steeper aerosol size distribution compared to the Arabian Sea, which could be either due to closer proximity to the source regions or due to large abundance or both.

The large values of  $a$  over the Bay of Bengal could be due to the direct impact of the anthropogenically influenced east coast of India (source of sub-micron aerosols). The smaller values of  $a$  over the Arabian Sea are probably due to the longer sea-travel of the corresponding air masses. Moreover, since the Arabian Sea is influenced by the northwest regions of the Indian sub-continent, it carries larger dust particles to the Arabian Sea which make the value of  $a$  smaller. Almost flat spectral variation of aerosol optical depth over the Indian Ocean is representative of the far oceanic regions.

#### *Effect of continental proximity*

In order to examine the effect of the continent on the aerosol optical depths, the values have been averaged over two regions. The first one is a region of the Bay of Bengal and the Arabian Sea which are closer to the con-

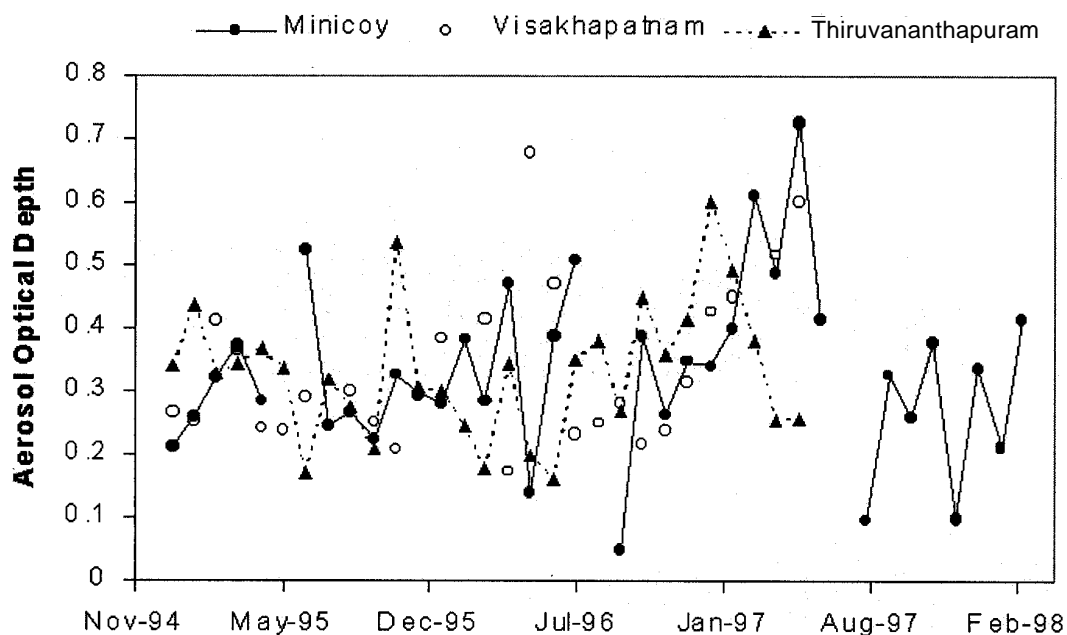


**Figure 8.** Long-term variation of the aerosol optical depth at 500 nm measured at three locations – Visakhapatnam (east coast of India), Thiruvananthapuram (southwest coast of India) and Minicoy (an island station in the Arabian Sea).

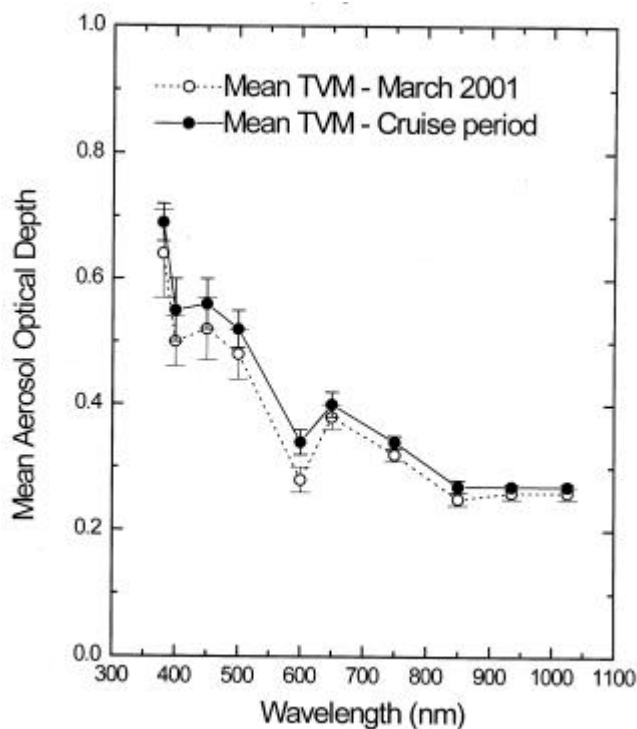


**Figure 9.** Spectral variation of  $\tau_p$  at Thiruvananthapuram. Continuous line with solid circles represents the mean  $\tau_p - I$  for the cruise period and dashed line with open circles represents the mean values for March 2001.

**Table 3.** Mean Angstrom coefficients for Thiruvananthapuram

$a^*$	$1.09 \pm 0.46$	$b^*$	0.235
$a_{\text{mean}}$	$0.94 \pm 0.05$	$b_{\text{mean}}$	0.25

continent and the second region is the equatorial Indian Ocean which is farther away from the continent, such that an air mass from the continent would take several days to reach there, under normal conditions. Figure 7 shows the spectral variation of aerosol optical depth averaged over these regions. The vertical bars represent the standard deviations. The large difference in the near UV and visible optical depths is clearly due to the small particle effect discussed earlier.

The features along the west coast of India have been investigated earlier (during INDOEX)<sup>20,27</sup>. Similar enhancement in the near UV and visible aerosol optical depths near the coast has been reported. Since this enhancement is mainly due to the anthropogenic aerosols, a similar observation over the Bay of Bengal should not come as a surprise. However, the higher values of  $a$  observed over the Bay of Bengal indicate a possible difference between the aerosol characteristics over the Bay of Bengal and those over the Arabian Sea.

### Comparison with inland and island observations

As a part of ISRO-GBP, continuous observations of aerosol optical depth have been made at different regions over continental India<sup>13</sup>. Here, we have compared the ship-borne data with these observations. Figure 8 shows the long-term variation of the aerosol optical depth at 500 nm measured at three locations – Visakhapatnam (east coast of India), Thiruvananthapuram (southwest coast of India) and Minicoy (an island station in the Arabian Sea). The climatological values are comparable with the present near-coastal observations.

During the cruise period, a multi-wavelength radiometer was in regular operation at Thiruvananthapuram (8.5°N, 77°E) on all clear days. The data collected from this represented the scenario that prevailed over the coastal region during the cruise time. Figure 9 shows the spectral variation of  $\tau_p$  at Thiruvananthapuram, where continuous line with solid circles represents the mean  $\tau_p - I$  for the cruise period and the dashed line with open circles represents the mean values for March 2001. The vertical bars are the standard errors. The spectral variation is typical of that observed for a remote continental coastal station and resembles quite well that seen over the Arabian Sea. The values of  $a$  and  $b$  are computed using the ten  $\tau_p - I$  values for all the individual days and the mean value of  $(aa^*)$  and  $(bb^*)$  are estimated.  $a$  and  $b$  are also estimated for the mean curve (solid) shown in Figure 9. These are listed in Table 3. It is seen that the values of  $a$  and  $a^*$  are very similar to those observed for the Arabian Sea, but are larger than those for the Bay of Bengal.

### Conclusions

1. The atmosphere over the Bay of Bengal was found to be more turbid than that over the Arabian Sea.
2. Aerosol optical depth decreases with distance from the coast with an e-folding *scale distance* of approximately  $\sim 1000$  km for near UV and visible wavelengths, and  $\sim 1600$  km for near IR wavelengths.
3. A comparison of the near-coastal values of aerosol optical depth with ocean values shows a large difference in near UV and visible wavelengths compared to near IR wavelengths, which clearly shows the relative dominance of small particles near the coast.
4. Trajectory analysis showed that the Bay of Bengal was mainly influenced by the eastern coast of India, the Indian Ocean mainly by the Indian subcontinent and the Arabian Sea by the northwest of India and countries lying northwest of India.



1. Charlson, R. J., Schwartz, S. E., Hales, J. M., Cess, R. D., Coakley, J. A., Hansen, J. E. and Hoffmann, D. J., *Science*, 1992, **255**, 423–430.
2. Andreae, M. O., in *World Survey of Climatology, Future Climates of the World* (ed. Henderson-Sellers, A.), Elsevier, New York, 1995, vol. 16, pp. 341–392.
3. Kaufman, Y. J. *et al.*, *J. Geophys. Res.*, 1998, **103**, 31783–31808.
4. d'Almeda, G. A., Koepke, P. and Shettle, E. P., *Atmospheric Aerosols – Global Climatology and Radiative Characteristics*, A. Deepak, Hampton, Va, 1991.
5. Satheesh, S. K. *et al.*, *J. Geophys. Res.*, 1999, **104**, 27421–27440.
6. Satheesh, S. K. and Ramanathan, V., *Nature*, 2000, **405**, 60–63.
7. Ramanathan, V. *et al.*, Indian Ocean Experiment (INDOEX) White Paper, C<sup>4</sup>, Scripps Institution of Oceanography, La Jolla, California, 1995.
8. Intergovernmental Panel on Climate Change, Report to IPCC from the Scientific Assessment Group (WGI), Cambridge Univ. Press, New York, 1995.
9. Coakley, J. A. and Cess, R. D., *J. Atmos. Sci.*, 1985, **42**, 1677–1692.
10. Bates, T. S. *et al.*, *J. Geophys. Res.*, 1998, **103**, 16297–16318.
11. Raes, F. *et al.*, *Tellus*, 2000, **52B**, 111–125.
12. Russell, P. B. *et al.*, *J. Geophys. Res.*, 1999, **104**, 2289–2307.
13. Moorthy, *et al.*, Aerosol Climatology over India I – ISRO GBP MWR Network and Database, ISRO GBP SR-03-99, 1999.
14. Subbaraya, *et al.*, *J. Indian Geophys. Union*, 2000, **4**, 77–90.
15. Moorthy, K. K. and Satheesh, S. K., *Q. J. R. Meteorol. Soc.*, 2000, **126**, 81–109.
16. Bhat, G. S. *et al.*, *Bull. Am. Meteorol. Soc.*, 2001 (in press).
17. Das, P. K., 5th IMO Lecture, WMO No. 613, 1986.
18. Shaw, G. E., Regan, J. A. and Herman, B. M., *J. Appl. Meteorol.*, 1973, **12**, 374–380.
19. Moorthy, K. K., Satheesh, S. K. and Krishna Murthy, B. V., *J. Geophys. Res.*, 1997, **102**, 18827–18842.
20. Satheesh, S. K. and Krishna Moorthy, K., *Tellus*, 1997, **49B**, 417–428.
21. Krishnamurti, T. N., Jha, B., Prospero, J. M., Jayaraman, A. and Ramanathan, V., *Tellus*, 1998, **50B**, 521–542.
22. Moorthy, K. K. and Saha, A., *J. Atmos. Sol.-Terr. Phys.*, 2000, **62**, 65–72.
23. Satheesh, S. K., Krishna Moorthy, K. and Krishna Murthy, B. V., *J. Geophys. Res.*, 1998, **103**, 26183–26192.
24. Moorthy, *et al.*, *J. Geophys. Res.*, 2001 (in press).
25. Angstrom, A., *Tellus*, 1961, **13**, 214–223.
26. Moorthy, K. K., Satheesh, S. K. and Murthy, B. V. K., *J. Atmos. Sol.-Terr. Phys.*, 1998, **60**, 981–992.
27. Jayaraman, A., Lubin, D., Ramachandran, S., Ramanathan, V., Woodbridge, E., Collins, W. and Zalpuri, K. S., *J. Geophys. Res.*, 1998, **103**, 13827–13836.

ACKNOWLEDGEMENTS. We thank Prof. J. Srinivasan and Prof. G. S. Bhat of Centre for Atmospheric and Oceanic Sciences for making our participation in the cruise possible, and for useful discussions which improved the quality of the paper significantly.

We also thank the active support from Mr Duli Chand of Physical Research Laboratory during the experiment. Thanks are also due to Mr Suresh Babu of Space Physics Laboratory for conducting MWR observations at Thiruvananthapuram, simultaneously with the cruise period. Logistical support received from Dr M. Sudhakar of NCOAR, Goa to conduct the experiment is also acknowledged.

The trajectories are estimated using Hysplit trajectory model of NOAA.

Received 8 June 2001; revised accepted 28 September 2001